Assessing the influence of transect interval in monitoring and analysis of shoreline change

T.W.S. Warnasuriya (sameethocg@gmail.com)
Ocean University of Sri Lanka

Research Article

Keywords: Beach morphology, Remote Sensing, DSAS, Google Earth, GIS

Posted Date: July 29th, 2022

DOI: https://doi.org/10.21203/rs.3.rs-1842868/v1

Additional Declarations: No competing interests reported.

Version of Record: A version of this preprint was published at Environmental Monitoring and Assessment on April 3rd, 2023. See the published version at https://doi.org/10.1007/s10661-023-11161-5.

Abstract

Shoreline analysis helps to understand the coastal dynamism for decision making in coastal management. As there are still doubts in transect-based analysis, this study attempts to understand the influence of transect intervals in shoreline analysis. Shorelines were delineated on high-resolution satellite images in Google Earth Pro for twelve beaches in Sri Lanka under different spatial and temporal scales. Shoreline change statistics were calculated using Digital Shoreline Analysis System in ArcGIS 10.5.1 software under 50 transect interval scenarios and influence of the transect interval for shoreline change statistics were interpreted using standard statistical methods. Transect Interval Error was calculated with respect to the 1 m scenario as this has the best beach representation. Results revealed that there is no any significant difference ($p > 0.05$) of shoreline change statistics between 1 m scenarios and 50 m scenario in each beach. Further, it was found that the error was extremely low up to 10 m scenario and then after it was subject to fluctuate in an unpredictable manner ($R2 < 0.5$). Overall, the study concludes that the influence of the transect interval is negligible and 10 m transect interval is ideal in shoreline analysis for the highest efficacy in small sandy beaches.

Introduction

The shoreline can be considered as one of the most dynamic boundaries (Mukhopadhyay et al. 2012; Hapke et al. 2011; Rongxing Li, Liu, and Felus 2001) in the coastal environment laid between land and water (Boak and Turner 2005) which is frequently subject to short-term (Ali and Narayana 2015) or long-term changes (Fenster, Dolan, and Morton 2001). This dynamism can occur from both natural activities such as wind, currents, tides, waves, sea-level rise, extreme events etc. (Quashigah, Addo, and Kodzo 2013; Pajak and Leatherman 2002; Ali and Narayana 2015) and anthropogenic activities such as human constructions, sand mining etc. (Rongxing Li, Ma, and Di 2002; Oyedotun, Ruiz-Luna, and Navarro-Hernández 2018) and is observable in sandy beaches under the states of accretion or erosion (Abeykoon et al. 2021; Dolan, Fenster, and Holme 1991). Further, it has been identified that the 24% of the sandy beaches in the world are eroding at the rate exceeding 0.5 m/year (Luijendijk et al. 2018). This unprecedented coastal change could influence greatly on social, environmental and economic aspects (Fleming et al. 2018; Ervita and Marfai 2017; Quante and Colijin 2016) of the community directly or indirectly. Gradually, this can grow up to a global issue as an ample amount of people is concentrated in the vicinity of beaches in most parts of the world as a result of the population growth and the resources depletion (Crowell et al. 2007).

Definition, scale, method and accuracy are key concerns in shoreline mapping (Yao et al. 2015; Dang et al. 2018; Dewidar and Frihy 2010) as they determine the reliability of the study. Shoreline position has been defined in many ways such as land-water line, dry-wet line, vegetation line etc. (Gens 2010; Boak and Turner 2005) corresponding to a pre-defined datum (Liu, Sherman, and Gu 2007; Boak and Turner 2005). Tide-coordinated shorelines were also used in some studies when shorelines were defined in order to mitigate the errors introduced from tidal actions (Ron Li, Di, and Ma 2001; Hapke et al. 2011; Rongxing Li, Ma, and Di 2002).

Many shoreline research studies have focused on regional, national and global scales (Bertacchini and Capra 2010; Abeykoon et al. 2021; Luijendijk et al. 2018) compared to the local scale mapping (Warnasuriya et al. 2020; Warnasuriya, Gunaalan, and Gunasekara 2018). Therefore, understanding the shoreline dynamism under local scale (in small beaches or pocket beaches) mapping has found to be very important (Warnasuriya et al. 2020) in terms of coastal zone management (Elnabwy et al. 2020; Chen et al. 2005; Boateng, Wiafe, and Jayson-Quashigah 2017) and disaster management perspectives (Baig et al. 2020).

However, it is not an easy task to determine the temporal and spatial changes of individual beaches in a comprehensive basis due to its high heterogeneity, high complexity and high dynamism (Warnasuriya et al. 2020). On the other hand, conventional field surveys are very expensive, time consuming and labor intensive (Liu, Sherman, and Gu 2007; Warnasuriya, Kumara, and Alahacoon 2014; Natesan et al. 2013). But, continuous monitoring is needed to understand and interpret the characteristics of beaches and their dynamisms properly (Makota, Sallema, and Mahika 2004; Sesli et al. 2009; White and El Asmar 1999). Nevertheless, understanding the coastal dynamism is a challenging task with the existing scientific method in terms of effectiveness, efficiency and reliability (Warnasuriya et al. 2020).

It has been identified that the using remote sensing and GIS techniques is very popular in shoreline studies (Liu, Sherman, and Gu 2007; Zagórski, Jarosz, and Superson 2020; Appeaning Addo, Jayson-Quashigah, and Kufogbe 2012; Nassar et al. 2019; Niya et al. 2013; Ahmad and Lakhan 2012; Yasir et al. 2020), because they provide platforms to execute shoreline change analysis effectively and efficiently (Warnasuriya et al. 2020) over the conventional field surveys (Lipakis, Chrysoulakis, and Kamarianakis 2005). Remote sensing technology has been widely used in shoreline studies (Toure et al. 2019) during past few decades through aerial photography (Rongxing Li et al. 2008; Chaaban et al. 2012; Ford 2013), satellite imagery (Baig et al. 2020; Elnabwy et al. 2020), LiDAR technology (Terefenko et al. 2019) and Drone photography (Lowe et al. 2019). However, still satellite images are very popular among the scientists as they are readily available in the most cases compared to the other aforementioned remote sensing techniques.

Image resolution is one of the key factors to be considered when extracting information under different mapping scales. As far as the accuracy is concerned, high-resolution satellite images (Warnasuriya, Gunaalan, and Gunasekara 2018; Ford 2013; Warnasuriya et al. 2020) are found to be more effective in shoreline studies under local scale mapping (large-scale maps) in small beaches which can be considered as pocket beaches. But, availability of such high-resolution satellite images is limited for the most studies due to high cost and limited coverage. Currently, there are satellite images available even around 30 cm spatial resolution obtained specially from latest Worldview satellites. Other than that, high-resolution images are provided by the satellites; GeoEye, QuickBird, IKONOS, SPOT, Pleiades etc. They provide satellite images with spatial resolution from 0.31 m to 2.00 m (Warnasuriya, Gunaalan, and Gunasekara 2018; Warnasuriya et al. 2020). Google Earth Pro has been found as an ideal source for high-resolution satellite images as it provides some of them for free of charge under the maximum zoom level and it updates time to time with new high-resolution satellite images. Although the spatial resolution is

not given for high-resolution images in Google Earth platform, this was inferred by Warnasuriya et al. in 2018 and 2020 referring to the original sources of image provider such as Maxar technologies (previously Digital Globe), CNES/Airbus etc. and considering minimum possible identifiable features from the images.

However, it is not just enough to have high-resolution images unless there is a proper mechanism to quantify shoreline changes. Dolan et al in 1991 introduced some Shoreline Change Statistics (SCS) which are very helpful to analyze shoreline changes quantitatively. Later these methods have been incorporated into Digital Shoreline Analysis System (DSAS) developed by USGS (Himmelstoss et al. 2018) which is one of the widely used software for shoreline change analysis in the recent past (Oyedotun, Ruiz-Luna, and Navarro-Hernández 2018; Baig et al. 2020). Warnasuriya et al. also tried to develop new methods and considerations for shoreline change analysis by means of DSAS and Google Earth Pro in 2018 and 2020. According to those studies, it was identified that resolution, eye-altitude, digitizing error, georeferencing error (shift error), tidal error, wave runup error and zonation are key influential factors in shoreline uncertainties. But, still there are some factors to be further evaluated in transect based shoreline change analysis with regard to coastal morphology and selected transect intervals when interpreting the overall statistics for individual beaches. Therefore, this study attempts to understand the influence of those factors on SCS under different transect interval scenarios.

Materials And Methods

Study area

The study was carried out in twelve sandy beaches which are recreationally important in southern coast of Sri Lanka (Figure 1). Specifications of each beach are given in the Table 1.

Data collection

Shorelines were delineated from Google Earth Pro software on time series high-resolution satellite images for aforementioned twelve beaches (Table 1) having three different morphological features namely convex, concave and straight (Figure 2) representing four beaches for each category. They were manually digitized referring to the land-water boundary (instantaneous shoreline) under 300 m eye-altitude (Warnasuriya et al. 2020). Then all the digitized shorelines were saved as Keyhole Markup Language (KML) file format. The major reason for the selection of land-water boundary as the instantaneous shoreline in this study is that this is the most identifiable and convenient line to be visualized from high-resolution satellite images from Google Earth Pro.

Table 1. Specification of the delineated shorelines

Beach	Year range	No. of shorelines	Approximate length (m)	Latitude	Longitude	Beach morphology
Pareiwella	2003-2020	14	174	6.022800°	80.800768°	Convex
Polhena	2005-2020	28	177	5.936192°	80.526007°	Convex
Galle fort	2002-2020	23	362	6.024602°	80.219759°	Convex
Weligama	2005-2020	23	400	5.959403°	80.421676°	Convex
Ussangoda	2003-2020	14	716	6.092852°	80.986199°	Concave
Dikwella	2006-2020	16	484	5.960113°	80.684232°	Concave
Mirissa	2005-2020	23	1049	5.944701°	80.459139°	Concave
Unawatuna	2002-2020	26	1272	6.009405°	80.247881°	Concave
Hikkaduwa	2003-2020	22	1108	6.137365°	80.099051°	Straight
Kalamatiya	2009-2019	14	5857	6.085899°	80.953386°	Straight
Rekawa	2005-2020	18	4256	6.044914°	80.843008°	Straight
Koggala	2002-2020	26	4011	5.992579°	80.310814°	Straight

Note: Information in this table was derived from Google Earth Pro. Spatial resolution is between 0.31 m to 2.00 m as evident in Warnasuriya et al. 2020.

Data processing

Shorelines in KML format were converted into shapefile (.shp) from ArcGIS 10.5.1 software and saved them in a personal geodatabase. They were projected in WGS 84 –UTM –zone 44N projection and ensured the appropriate appending of shorelines in each beach. Date field and Uncertainty field were added to the attribute table of each set of shorelines and the data were fed appropriately. Uncertainty was assumed as zero in this study as this is not a key consideration in this study. But, it is very important to consider the uncertainty due to georeferencing, tidal effect, wave action and human error due to digitizing when interpreting coastal geomorphological changes. It was identified that the uncertainty of shoreline studies using Google earth is about 9.06±3.15 (Warnasuriya et al. 2020). A baseline was created for each

beach manually at landside to have the best representation of the appended shorelines for each beach. Then digital transects were cast under 50 different Transect Interval Scenarios (TISs) from 1 m to 50 m with 1m gap (1 m, 2 m, 3 m, ……., 50 m) for each beach using DSAS 5.0 tool in ArcGIS 10.5.1 software (Figure 3). TISs were limited up to 50 m because the smallest beach has the length of 174 m which can occupy at least two or three transects and when increasing the TISs, number of replicates can be reduced up to one. Each TIS was then used to calculate SCS for each beach.

Data analysis

Data were analyzed using the DSAS 5.0 tool in ArcGIS 10.5.1 software to calculate SCS such as Shoreline Change Envelope (SCE), Net Shoreline Movement (NSM), End Point Rate (EPR) and Linear Regression Rate (LRR) for each TIS under each beach (Himmelstoss et al. 2018). Descriptive statistics such as Average, Standard Deviation (SD), Maximum (Max.) and Minimum (Min.) values were also calculated for each TIS under each beach using MS Excel 2016 software. Then the average values of each SCS (dependent variable) were plotted against the transect interval (independent variable) and subsequently, the regression analysis was implemented for each beach using MS Excel 2016 software to understand whether there are clear trends of SCS with the TISs or not. Independent sample T-test was applied to check whether there is a significant difference of SCS between Most Beach Representative Scenario (MBRS) and Least Beach Representative Scenario (LBRS) from SPSS 16.0 software. 1 m TIS was considered as the MBRS assuming the 100% representation of the beach while 50 m TIS was considered as the LBRS representing 2% of the beach with respect to the MBRS. Error of the Average Shoreline Change Statistics (ASCS) in each TIS was calculated with respect to the ASCS of MBRS (reference value in the error estimation) for each beach (Eq. (1)) and this error was named as Transect Interval Error (TIE). Note that when the reference value is a plus value, overestimations are denoted by plus values while underestimations are denoted by minus values in the results derived from the Eq. 1. But, when the reference value is a minus value, overestimations are denoted by minus values while underestimations are denoted by plus values in the results derived from the Eq.1.

$$Transect\ Interval\ Error\ (TIE) = Xi - X \qquad (1)$$

Where, Xi is the ASCS (SCE or NSM or EPR or LRR) in i^{th} TIS and X is the ASCS of MBRS which is the reference value in this error estimation.

This error (TIE) was also plotted against the transect interval to understand the pattern of error change with the increasing of TISs. The descriptive statistics were also calculated to estimate Average, SD, Max. and Min. values of the error in each beach. One-Way ANOVA statistical test was applied in SPSS 16.0 software to check whether there is a significant difference in TIE of ASCS among the beaches with and without considering the beach morphology. Null hypothesis in this regard is ‘there is no any significant difference in TIE among beaches in terms of ASCS’ and the alternative hypothesis is the opposite of that. Further, the average TIE of each ASCS were compared under five different scenarios namely, first 10 m,

first 20 m, first 30 m, first 40 m and first 50 m to understand the best transect interval range to be selected in transect based shoreline change analysis. Flow chart of the methodology is given in Figure 4.

Results And Discussion

Average Shoreline Change Statistics (ASCS) showed that some fluctuations were observed under different Transect Interval Scenarios (TISs) with respect to the Most Beach Representative Scenario (Table 2). Changing patterns of the ASCS; SCE (Figure 5), NSM (Figure 6), EPR (Figure 7), LRR (Figure 8) against the TIS are different among beaches and they are unpredictable. Regression values of each graph (Figure 5-8) also tells us that there are no any definite trends of ASCS ($R^2 < 0.5$).

Table 2. ASCS of MBRS as the reference value used in the error estimation for each beach

Beach	SCE (m)	NSM (m)	EPR (m/year)	LRR (m/year)
Pareiwella	35.15±8.99	0.05±7.5	0.003±0.46	-0.47±0.37
Polhena	28.87±5.77	1.35±13.95	0.09±0.93	0.0004±0.92
Galle Fort	12.52±4.16	1.25±4.62	0.07±0.26	0.18±0.37
Weligama	37.78±14.36	28.2±25.45	1.98±1.79	1.16±1.22
Ussangoda	17.09±4.53	-2.19±5.94	-0.13±0.35	0.12±0.33
Dikwella	13.36±2.83	-5.59±3.17	-0.39±0.22	-0.29±0.2
Mirissa	38.71±8.01	2.7±8.01	0.18±0.53	0.07±0.17
Unawatuna	50.56±8.51	15.8±13.87	0.89±0.78	1.88±0.82
Hikkaduwa	27.27±7.23	-8.31±12.14	-0.49±0.72	-0.3±0.76
Kalamatiya	46.83±13.15	17.03±21.54	1.77±2.24	0.11±1.27
Rekawa	39.04±12.81	4.64±30.47	0.31±2.17	0.17±1.18
Koggala	50.83±18.44	-7.48±10.09	-0.42±0.57	0.09±0.64

Note: Minus values are erosions and plus values are accretions

Overall, the scatter plots (Figure 5-8) show that when increasing transect intervals, dispersion of the ASCS values is also increased. But, there are many cases showed almost similar values at the tail end of the TISs with respect to the MBRS. This indicates that transect interval doesn't always influence on ASCS in small beaches in a similar way. Interestingly, it was further observed that some beaches such as Pareiwella (Figure 6a, 7a) and Polhena (Figure 6b, 7b, 8b) had both positive (accretion) and negative (erosion) values of NSM, EPR and LRR for different TISs. This situation can mislead the interpretation when describing the overall status of beach in terms of accretion or erosion. However, the descriptive statistics (Table 3 and 4) showed that the measure of dispersion (such as SD and range) of the SCS is

negligible for almost all the beaches with slight exceptions in Pareiwella, Polhena and Weligama beaches at times. This was further proved by the independent sample T-test (Table 5) as there was no any significant difference (P > 0.05) between the MBRS and the LBRS in each beach. In terms of beach physical processes, all the beaches can be considered as reflective beaches representing high (Pareiwella, Ussangoda, Dikkwella, Kalamatiy and Rekawa) and moderate (Polhena, Galle Fort, Weligama, Mirissa, Unawatuna, Hikkaduwa and Koggala) energy zones according to the Sri Lankan wave climate. High energy zone is defined as the places where the wave height is from 0.6 m to 3.5 m while the moderate energy zone having the wave height from 0.3 m to 3.3 m (Survey Department of Sri lanka 2007). Tide variation for all the beaches are between 0.4 m and 0.6 m.

Table 3. Descriptive statistics for SCE and NSM in each beach

Beach	SCE (m)				NSM (m)			
	Mean	SD	Max.	Min.	Mean	SD	Max.	Min.
Paraiwella	36.24	4.61	47.98	29.08	-0.75	3.62	3.48	-10.23
Polhena	29.47	1.47	33.19	26.84	1.39	1.43	5.54	-1.85
Galle fort	12.58	0.37	13.85	11.83	1.54	0.42	2.89	0.92
Weligama	38.07	2.40	44.89	34.00	28.33	2.78	34.96	20.36
Ussangoda	17.05	0.24	17.78	16.27	-1.71	0.25	-0.91	-2.33
Dikwella	13.37	0.17	13.86	12.94	-5.65	0.25	-5.11	-6.63
Mirissa	38.65	0.25	39.42	37.94	2.66	0.16	3.16	2.29
Unawatuna	50.53	0.19	50.93	49.98	15.76	0.19	16.13	15.03
Hikkaduwa	27.35	0.27	28.43	26.93	-8.33	0.32	-7.53	-9.11
Kalamatiya	46.73	0.50	47.68	45.05	17.11	0.45	18.40	15.97
Rekawa	38.43	0.52	39.76	36.26	-4.77	1.09	-0.25	-7.09
Koggala	50.85	0.14	51.29	50.53	-7.45	0.13	-7.15	-7.78

Note: Minus values are erosions and plus values are accretions

Table 4. Descriptive statistics for EPR and LRR in each beach

Beach	EPR (m)				LRR (m)			
	Mean	SD	Max.	Min.	Mean	SD	Max.	Min.
Paraiwella	-0.05	0.22	0.21	-0.63	-0.45	0.13	-0.2	-0.69
Polhena	0.09	0.09	0.37	-0.12	-0.02	0.09	0.27	-0.21
Galle fort	0.09	0.029	0.169	0.05	0.20	0.02	0.28	0.17
Weligama	1.99	0.19	2.45	1.43	1.16	0.13	1.45	0.82
Ussangoda	-0.001	0.0005	0	-0.003	-0.001	0.0004	0	-0.002
Dikwella	-0.40	0.02	-0.36	-0.47	-0.29	0.009	-0.26	-0.31
Mirissa	0.18	0.01	0.21	0.15	0.07	0.008	0.08	0.05
Unawatuna	0.89	0.01	0.91	0.85	1.87	0.01	1.89	1.85
Hikkaduwa	-0.49	0.02	-0.44	-0.54	-0.30	0.02	-0.25	-0.35
Kalamatiya	1.78	0.05	1.92	1.66	0.10	0.03	0.17	0.01
Rekawa	-0.33	0.08	-0.02	-0.50	-0.23	0.03	-0.08	-0.31
Koggala	-0.42	0.007	-0.40	-0.44	0.10	0.005	0.12	0.09

Note: Minus values are erosions and plus values are accretions

Table 5. Independent sample T-test significant values (P) between 1m and 50m scenarios

Beach	SCE	NSM	EPR	LRR
Paraiwella	0.054	0.066	0.067	0.529
Polhena	0.823	0.812	0.81	0.767
Galle fort	0.803	0.587	0.591	0.885
Weligama	0.965	0.865	0.864	0.818
Ussangoda	0.713	0.892	0.889	0.987
Dikwella	0.984	0.989	0.998	0.961
Mirissa	0.953	0.963	0.964	0.81
Unawatuna	0.788	0.974	0.972	0.94
Hikkaduwa	0.874	0.868	0.864	0.901
Kalamatiya	0.973	0.767	0.767	0.708
Rekawa	0.92	0.827	0.82	0.864
Koggala	0.95	0.767	0.772	0.906

However, TIE of the ASCS revealed that under some TISs there were small overestimations while there were small underestimations in the other TISs (Table 6).

Table 6. Average TIE within 50 m TISs in each beach

Beach	SCE (m)	NSM (m)	EPR (m/year)	LRR (m/year)
Pareiwella	1.09±4.61	-0.8±3.62	-0.05±0.22	0.02±0.13
Polhena	0.6±1.47	0.05±1.43	0.003±0.09	-0.03±0.09
Galle Fort	0.05±0.38	0.29±0.42	0.02±0.02	0.02±0.02
Weligama	0.29±2.4	0.14±2.78	0.009±0.19	0.005±0.13
Ussangoda	-0.04±0.24	4.3E-06±0.3	0.0003±0.02	0.0003±0.01
Dikwella	0.01±0.17	-0.06±0.24	-0.004±0.02	-0.002±0.009
Mirissa	-0.06±0.25	-0.03±0.16	-0.002±0.01	-0.002±0.008
Unawatuna	-0.03±0.19	-0.05±0.19	-0.003±0.01	-0.002±0.01
Hikkaduwa	0.08±0.27	-0.02±0.32	-0.001±0.02	-0.00074±0.02
Kalamatiya	-0.095±0.5	0.078±0.45	0.008±0.05	-0.0047±0.03
Rekawa	0.014±0.25	-0.04±0.32	-0.003±0.02	-0.002±0.01
Koggala	0.03±0.14	0.03±0.13	0.001±0.007	0.002±0.005

Table 7. Average TIE within 50 m TISs in each beach morphology

Beach	SCE (m)	NSM (m)	EPR (m/year)	LRR (m/year)
Convex	0.51±0.45	-0.08±0.49	-0.005±0.03	0.005±0.02
Concave	-0.03±0.03	-0.04±0.03	-0.002±0.002	-0.002±0.001
Straight	0.008±0.08	0.01±0.05	0.001±0.005	-0.001±0.003

Out of all beaches, Pareiwella beach had the most uncertainty in shoreline change analysis with average TIE values; 1.09±4.61 m, -0.8±3.62 m, -0.05±0.22 m/year and 0.02±0.13 m/year for SCE, NSM, EPR and LRR respectively while the least uncertainty is varied among the beaches with respect to ASCS (Table 6). When the beach morphology is considered, it was identified that the highest average TIE was given by the convex-beach while the lowest of that is given by the straight-beach (Table 7). The highest overestimation of SCE was observed in Pareiwella beach (12.83 m) under the transect interval 50 m while the lowest overestimation was also observed in Pareiwella beach (0.0007 m) under the transect interval 2 m. The highest underestimation of SCE was also observed in Pareiwella beach (-6.06 m) under the transect interval 30 m while the lowest underestimation was observed in Unawatuna beach (-0.00025 m) under the transect interval 10 m (Figure 9; Table 8).

Table 8. Overestimation and underestimation of SCE in each beach

Beach	Max. overestimation	Max. underestimation	Min. overestimation	Min. underestimation
Pareiwella	12.83	-6.06	0.000704	-0.2139
Polhena	4.31	-2.035	0.010118	-0.00912
Galle Fort	1.32	-0.69	0.00695	-0.00355
Weligama	7.11	-3.77	0.036059	-0.13581
Ussangoda	0.68	-0.82	0.005005	-0.02676
Dikwella	0.5	-0.41	0.001055	-0.00791
Mirissa	0.71	-0.76	0.01002	-0.0083
Unawatuna	0.36	-0.58	0.00518	-0.00025
Hikkaduwa	1.16	-0.34	0.004045	-0.00225
Kalamatiya	0.85	-1.77	0.017258	-0.00613
Rekawa	0.67	-0.85	0.002372	-0.0072
Koggala	0.46	-0.3	0.000971	-0.00091

The highest overestimation of NSM was observed in Weligama beach (6.75 m) under the transect interval 34 m while the lowest overestimation was observed in Rekawa beach (0.00016 m) under the transect interval 3 m. The highest underestimation of NSM was observed in Pareiwella beach (-10.27 m) under the transect interval 50 m while the lowest underestimation was observed in Koggala beach (0.000171 m) under the transect interval 2 m (Figure 9; Table 9).

Table 9. Overestimation and underestimation of NSM in each beach

Beach	Max. overestimation	Max. underestimation	Min. overestimation	Min. underestimation
Pareiwella	3.43	-10.27	0.138417	-0.11632
Polhena	4.19	-3.19	0.016078	-0.09402
Galle Fort	1.64	-0.33	0.005542	-0.01317
Weligama	6.75	-7.83	0.049536	-0.07129
Ussangoda	-0.97	0.67	-0.00709	0.008869
Dikwella	-1.03	0.47	-0.00075	0.000937
Mirissa	0.46	-0.40	0.001549	-0.00095
Unawatuna	0.32	-0.78	0.003911	-0.00052
Hikkaduwa	-0.79	0.78	-0.002	0.001003
Kalamatiya	1.37	-1.06	0.016104	-0.00165
Rekawa	0.91	-0.80	0.00016	-0.0039
Koggala	-0.30	0.32	-0.00047	0.000171

The highest overestimation of EPR was observed in Weligama beach (0.47 m/year) under the transect interval 34 m while the lowest overestimation was observed in Koggala beach (-4.9x 10^{-5} m/year) under the transect interval 2 m The highest underestimation of EPR was observed in Pareiwella beach (-0.62 m/year) under the transect interval 50 m while the lowest underestimation was observed in Dikwella beach (6.91 x 10^{-5} m/year) under the transect interval 2 m (Figure 10; Table 10).

Table 10. Overestimation and underestimation of EPR in each beach

Beach	Max. overestimation	Max. underestimation	Min. overestimation	Min. underestimation
Pareiwella	0.21	-0.62	0.0083	-0.00842
Polhena	0.28	-0.21	0.000686	-0.00637
Galle Fort	0.09	-0.01	0.000274	-0.00164
Weligama	0.47	-0.54	0.002952	-0.00505
Ussangoda	-0.05	0.04	-0.0003	0.000487
Dikwella	-0.07	0.03	-0.00013	6.91E-05
Mirissa	0.03	-0.02	0.000314	-0.00026
Unawatuna	0.01	-0.04	0.00028	-9.5E-05
Hikkaduwa	-0.046	0.04	-0.00033	0.0007
Kalamatiya	0.14	-0.11	0.00155	-0.00017
Rekawa	0.06	-0.05	0.000122	-0.00031
Koggala	-0.01	0.01	-4.9E-05	0.000103

The highest overestimation of LRR was observed in Weligama beach (0.29 m/year) under the transect interval 34 m while the lowest overestimation was observed in Koggala beach (2.64×10^{-5} m/year) under the transect interval 7 m. The highest underestimation of LRR was observed in Weligama beach (-0.34 m/year) under the transect interval 36 m while the lowest underestimation was observed in Unawatuna beach (1.3×10^{-5} m/year) under the transect interval 26 m (Figure 10; Table 11).

Table 11. Overestimation and underestimation of LRR in each beach

Beach	Max. overestimation	Max. underestimation	Min. overestimation	Min. underestimation
Pareiwella	-0.21	0.27	-0.00453	0.001043
Polhena	0.26	-0.21	0.004608	-0.00451
Galle Fort	0.09	-0.01	0.000341	-8.4E-05
Weligama	0.29	-0.34	0.003408	-0.00158
Ussangoda	0.04	-0.04	0.000482	-5.4E-05
Dikwella	-0.02	0.02	-8.7E-05	1.42E-05
Mirissa	0.011	-0.02	7.81E-05	-0.00011
Unawatuna	0.01	-0.02	0.000502	-1.3E-05
Hikkaduwa	-0.04	0.04	-0.00163	0.000303
Kalamatiya	0.06	-0.09	0.000274	-0.00045
Rekawa	0.03	-0.05	0.000375	-0.00089
Koggala	0.02	-0.0068	2.64E-05	-6.4E-05

According to the One-Way ANOVA test, there was a significant difference ($P < 0.05$) in the TIE of SCE while there was no any significant difference ($P > 0.05$) in the TIE of NSM, EPR and LRR among all the beaches without morphological consideration (all the beaches were simultaneously considered). It was identified that there was no any significant difference ($P > 0.05$) in the TIE of ASCS (SCE, NSM, EPR and LRR) in convex (Pareiwella, Polhena, Galle Fort and Weligama) and concave (Ussangoda, Dikwella, Mirissa and Unawatuna) morphologies. Although, the TIE of the ASCS such as NSM, EPR and LRR in Straight beaches had no significant difference ($P > 0.05$), there was a significant difference ($P < 0.05$) in TIE of SCE among the beaches represent the straight (Hikkaduwa, Kalamatiya, Rekawa and Koggala) morphology (Table 12).

Table 12. Results of the ANOVA test for TIE difference among beaches under different scenarios

Individual beach as one category				
Statistics	**P-value**	**Significance**	**Null hypothesis**	**Categories used in ANOVA test**
SCE	0.006	Different	Reject	Pareiwella, Polhena, Galle Fort, Weligama, Ussangoda, Dikwella, Mirissa, Unawatuna, Hikkaduwa, Kalamatiya, Rekawa, Koggala
NSM	0.065	No	Accept	
EPR	0.118	No	Accept	
LRR	0.57	No	Accept	
Beach morphology as one category				
SCE	0.001	Different	Reject	Convex, Concave, Straight
NSM	0.807	No	Accept	
EPR	0.795	No	Accept	
LRR	0.51	No	Accept	
Individual beach in one morphological feature as one category				
SCE	0.251	No	Accept	Convex (Pareiwella, Polhena, Galle Fort, Weligama)
NSM	0.104	No	Accept	
EPR	0.143	No	Accept	
LRR	0.107	No	Accept	
SCE	0.429	No	Accept	Concave (Ussangoda, Dikwella, Mirissa, Unawatuna)
NSM	0.604	No	Accept	
EPR	0.514	No	Accept	
LRR	0.597	No	Accept	
SCE	0.044	Different	Reject	Straight (Hikkaduwa, Kalamatiya, Rekawa, Koggala)
NSM	0.27	No	Accept	
EPR	0.214	No	Accept	
LRR	0.397	No	Accept	

However, the TIE was extremely low within the first 10m (Table 13-15) TISs while the error rapidly fluctuates when increasing the TISs in all the beaches for all ASCS (Figure 9-10). But, it was further observed that in some beaches under some ASCS, there were very close results between the MBRS and the LBRS as represents in Figure 5d, 5f, 5g, 5i, 6d, 6f, 7d, 7f, 8d, 8f, 8k, 8l etc.

Table 13. Average TIE of the first 10 m to first 50 m scenarios.

Scenario	SCE	NSM	EPR	LRR
First 10 m	0.018±0.032	-0.015±0.081	-0.00094±0.005	-0.001±0.005
First 20 m	0.024±0.113	0.051±0.14	0.0038±0.01	0.001±0.007
First 30 m	0.043±0.121	0.042±0.127	0.003±0.009	0.001±0.006
First 40 m	-0.025±0.22	0.065±0.209	0.004±0.013	-0.001±0.009
First 50 m	0.162±0.349	-0.035±0.26	-0.0019±0.016	0.0006±0.011

Table 14. Average TIE within first 10 m TISs in each beach

Beach	SCE (m)	NSM (m)	EPR (m/year)	LRR (m/year)
Pareiwella	0.05±0.34	-0.05±0.51	-0.003±0.03	-0.005±0.01
Polhena	0.04±0.13	-0.24±0.33	-0.02±0.02	-0.02±0.02
Galle Fort	0.006±0.05	0.001±0.05	7.83E-05±0.002	0.0005±0.003
Weligama	0.1±0.35	0.12±0.41	0.008±0.03	0.006±0.02
Ussangoda	-0.015±0.05	0.014±0.02	0.00096±0.002	0.00097±0.001
Dikwella	-0.00094±0.02	-0.002±0.01	-0.00012±0.001	4.17E-06±0.0008
Mirissa	0.011±0.05	-0.019±0.03	-0.0013±0.002	-0.00039±0.001
Unawatuna	0.014±0.02	0.014±0.03	0.0008±0.002	0.00086±0.002
Hikkaduwa	0.015±0.04	-0.03±0.08	-0.002±0.005	-0.0018±0.004
Kalamatiya	-0.011±0.05	0.015±0.03	0.002±0.003	-0.003±0.005
Rekawa	-0.004±0.03	-0.008±0.06	-0.00051±0.005	0.0006±0.002
Koggala	0.007±0.02	0.004±0.008	0.0002±0.0005	0.0003±0.0004

Table 15. Average TIE within first 10 m TISs in each beach morphology

Beach	SCE (m)	NSM (m)	EPR (m/year)	LRR (m/year)
Convex	0.05±0.04	-0.04±0.15	-0.003±0.01	-0.004±0.01
Concave	0.002±0.01	0.002±0.02	9.15E-05±0.001	0.0004±0.0007
Straight	0.002±0.01	-0.006±0.02	-0.0002±0.002	-0.0008±0.002

Although the errors are very low, when giving the overall status of the beach, it should be always used one of the better beach representative scenarios (1 m to 10 m) for highly complex beaches as there is a risk of misinterpretation whether the overall beach is subject to erode or accrete as Pareiwella and Polhena

beaches performed erosion and accretion in different TISs which was already described with respect to the Figures 6, 7 and 8 earlier. When compare TIE in ASCS among the three different morphological types of beaches (Table 7,15), it was identified that the TIE is high in the beach having the convex morphology with special reference to the Pareiwella beach compared to the other two morphological beach types. Warnasuriya et al. in 2020 found that the Pareiwella beach was drastically influenced by the 2004 Indian Ocean tsunami following a natural recovery up to a certain extent and this was also obvious from the shoreline distribution shown in Figure 2 for Pareiwella beach. Therefore, this can be the main reason for having high uncertainty when increasing the TISs. When the shorelines are influenced by extreme events such as tsunami (Ali and Narayana 2015), storms (Fenster, Dolan, and Morton 2001) etc., it is not ideal to use single baseline for shoreline change analysis as this doesn't help to cast transects representing the whole beach due to its heterogeneity. However, this type of issue was mitigated by Warnasuriya et al. in 2020 through zonation to describe the SCS for distinct zones creating different baselines according to the beach shape and aspect (morphology).

Conclusion

This study revealed that selected transect interval doesn't influence significantly on SCS in transect-based analysis with centimeter level uncertainties within 1 m to 50 m TISs for the small beaches with approximate length between 174 m to 5857 m irrespectively its beach morphology. Although the overall TIE is negligible, there are slight changes of the error of SCS among the three different beach morphologies. Convex beach performed highest error compared to the other two types namely concave and straight. Further, the study found that TIE was unpredicted with the increasing of the transect interval as there are many fluctuations at the tail end. As the result of this, overestimations and underestimations could be observed at times. Interestingly, the fluctuation of the error is very low within the first 10 m TISs. On the other hand, when comparing the error occurred from transect interval with digitizing error, shifting error and wave runup error (Warnasuriya et al. 2020), this TIE is negligible. But, when the error increased with the beach complexity, it is better to incorporate this error in shoreline change analysis to calculate the uncertainty. Although, 1 m is the MBRS, any transect interval can be selected between 1m to 50m for SCS giving the uncertainty. If the beach is highly complexed, it is better to select the transect interval within first 10m. This depends upon the required accuracy and the efficiency of the study. Normally, when processing large number of transects in DSAS, it takes more time to complete the calculation. Therefore, in big data analysis, this should be a key consideration. As far as the beach length is concerned, for long beaches it is possible to use transect intervals higher than 1m depending upon its complexity. However, it is important to implement a proper study to understand the shoreline complexity and develop relationship between TIE and shoreline complexity. Further, the influence of manually created baseline for transect orientation and SCS should also be evaluated in future studies. When giving the overall status of highly dynamic beaches in terms of erosion and accretion, it is better to use one of the TISs less than 10m. Findings of this study would be useful for the researchers when selecting the transect interval in shoreline studies in both computer-based and field-based analysis. Finally, the study would like to suggest to go for an integrated approach including transect-based, area-based (Anfuso et al. 2016) and volume-based

analyses, when carrying out comprehensive studies to interpret the beach dynamism by incorporating the shoreline uncertainty calculated from remote sensing, GIS and field survey technologies (Zagórski, Jarosz, and Superson 2020).

Declarations

Acknowledgements

I would like to convey the sincere thanks to the Ocean University of Sri Lanka for providing lab and library facilities.

Data Availability Statement

The datasets generated during and/or analysed during the current study are available from the corresponding author on reasonable request.

Statements and Declaration

No potential conflict of interest was reported by the author.

Funding

This research did not receive any specific grant from funding agencies in the public, commercial, or not-for-profit sectors.

References

1. Abeykoon, L.C.K., E.P.D.N. Thilakarathne, A. P. Abeygunawardana, T. W. S. Warnasuriya, and K. P. U. T. Egodauyana. 2021. “Are Coastal Protective Hard Structures Still Applicable With Respect to Shoreline Changes in Sri Lanka?” ADBI Working Paper Series. https://www.adb.org/publications/coastal-protective-hard-structures-still-applicable-shoreline-sri-lanka.
2. Ahmad, Sajid Rashid, and V. Chris Lakhan. 2012. “GIS-Based Analysis and Modeling of Coastline Advance and Retreat Along the Coast of Guyana.” Marine Geodesy 35 (1): 1–15. https://doi.org/10.1080/01490419.2011.637851.
3. Ali, P. Yunus, and A. C. Narayana. 2015. “Short-Term Morphological and Shoreline Changes at Trinkat Island, Andaman and Nicobar, India, After the 2004 Tsunami.” Marine Geodesy 38 (1): 26–39. https://doi.org/10.1080/01490419.2014.908795.
4. Anfuso, Giorgio, Dan Bowman, Chiara Danese, and Enzo Pranzini. 2016. “Transect Based Analysis versus Area Based Analysis to Quantify Shoreline Displacement: Spatial Resolution Issues.” Environmental Monitoring and Assessment 188 (10): 1–14. https://doi.org/10.1007/s10661-016-5571-1.

5. Appeaning Addo, K., P. N. Jayson-Quashigah, and K. S. Kufogbe. 2012. “Quantitative Analysis of Shoreline Change Using Medium Resolution Satellite Imagery in Keta, Ghana.” Marine Science 1 (1): 1–9. https://doi.org/10.5923/j.ms.20110101.01.
6. Baig, Mirza Razi Imam, Ishita Afreen Ahmad, Shahfahad, Mohammad Tayyab, and Atiqur Rahman. 2020. “Analysis of Shoreline Changes in Vishakhapatnam Coastal Tract of Andhra Pradesh, India: An Application of Digital Shoreline Analysis System (DSAS).” Annals of GIS 26 (4): 361–76. https://doi.org/10.1080/19475683.2020.1815839.
7. Bertacchini, Eleonora, and Alessandro Capra. 2010. “Map Updating and Coastline Control with Very High Resolution Satellite Images: Application to Molise and Puglia Coasts (Italy).” Italian Journal of Remote Sensing 42 (2): 103–15. https://doi.org/10.5721/ItJRS20104228.
8. Boak, Elizabeth H., and Ian L. Turner. 2005. “Shoreline Definition and Detection: A Review.” Journal of Coastal Research 21 (4): 688–703. https://doi.org/10.2112/03-0071.1.
9. Boateng, Isaac, George Wiafe, and Philip-Neri Jayson-Quashigah. 2017. “Mapping Vulnerability and Risk of Ghana’s Coastline to Sea Level Rise.” Marine Geodesy 40 (1): 23–39. https://doi.org/10.1080/01490419.2016.1261745.
10. Chaaban, Fadi, Hanan Darwishe, Yvonne Battiau-Queney, Barbara Louche, Eric Masson, Jamal El Khattabi, and Erick Carlier. 2012. “Using ArcGIS® Modelbuilder and Aerial Photographs to Measure Coastline Retreat and Advance: North of France.” Journal of Coastal Research 28 (6): 1567–79. https://doi.org/10.2112/JCOASTRES-D-11-00054.1.
11. Chen, Shui-sen, Liang-fu Chen, Qin-huo Liu, Xia Li, and Qiyu Tan. 2005. “Remote Sensing and GIS-Based Integrated Analysis of Coastal Changes and Their Environmental Impacts in Lingding Bay, Pearl River Estuary, South China.” Ocean & Coastal Management 48 (1): 65–83. https://doi.org/10.1016/j.ocecoaman.2004.11.004.
12. Crowell, Mark, Scott Edelman, Kevin Coulton, and Scott McAfee. 2007. “How Many People Live in Coastal Areas?” Journal of Coastal Research 23 (5). https://doi.org/10.2112/07A-0017.1.
13. Dang, Yamin, Chuanyin Zhang, Xinghua Zhou, Jun Xu, and Shuqiang Xue. 2018. “Instantaneous Shorelines as an Intermediate for Island Shoreline Mapping Based on Aerial/Satellite Stereo Images.” Marine Geodesy 41 (3): 219–29. https://doi.org/10.1080/01490419.2017.1397067.
14. Dewidar, Khalid M, and Omran E Frihy. 2010. “Automated Techniques for Quantification of Beach Change Rates Using Landsat Series along The.” Journal of Oceanography and Marine Science 1 (2): 28–39.
15. Dolan, Robert, Michael S Fenster, and Stuart J Holme. 1991. “Temporal Analysis of Shoreline Recession and Accretion.” Journal of Coastal Research 7 (3): 723–44.
16. Elnabwy, Mohamed T., Emad Elbeltagi, Mahmoud M. El Banna, Mohamed M.Y. Elshikh, Ibrahim Motawa, and Mosbeh R. Kaloop. 2020. “An Approach Based on Landsat Images for Shoreline Monitoring to Support Integrated Coastal Management - A Case Study, Ezbet Elborg, Nile Delta, Egypt.” ISPRS International Journal of Geo-Information 9 (4). https://doi.org/10.3390/ijgi9040199.

17. Ervita, Komariah, and Muh Aris Marfai. 2017. “Shoreline Change Analysis in Demak, Indonesia.” Journal of Environmental Protection 08 (08): 940–55. https://doi.org/10.4236/jep.2017.88059.
18. Fenster, Michael S., Robert Dolan, and Robert A. Morton. 2001. “Coastal Storms and Shoreline Change: Signal or Noise?” Journal of Coastal Research 17 (3): 714–20. http://www.jstor.org/stable/4300222%5Cnhttp://www.jstor.org/stable/pdfplus/4300222.pdf.
19. Fleming, Elizabeth, Jeffrey Payne, William V Sweet, Michael Craghan, John Haines, Juliette Finzi-Hart, Heidi Stiller, and Ariana Sutton-Grier. 2018. “Coastal Effects.” *Impacts, Risks, and Adaptation in the United States: Fourth National Climate Assessment, Volume II*. Vol. II. https://doi.org/10.7930/NCA4.2018.CH8.
20. Ford, Murray. 2013. “Shoreline Changes Interpreted from Multi-Temporal Aerial Photographs and High Resolution Satellite Images: Wotje Atoll, Marshall Islands.” Remote Sensing of Environment 135: 130–40. https://doi.org/10.1016/j.rse.2013.03.027.
21. Gens, R. 2010. “Remote Sensing of Coastlines: Detection, Extraction and Monitoring.” International Journal of Remote Sensing 31 (7): 1819–36. https://doi.org/10.1080/01431160902926673.
22. Hapke, Cheryl J, Emily A Himmelstoss, Metedith G Kratzmann, Jeffrey H List, and E Robert Thieler. 2011. “National Assessment of Shoreline Change: Historical Shoreline Change along the New England and Mid-Atlantic Coasts Open-File Report 2010–1118.” Virginia.
23. Himmelstoss, Emily A., Rachel E. Henderson, Meredith G. Kratzmann, and Amy S. Farris. 2018. “Digital Shoreline Analysis System (DSAS) Version 5.0 User Guide.” *Open-File Report 2018 – 1179*.
24. Li, Ron, Kaichang Di, and Ruijin Ma. 2001. “A Comparative Study of Shoreline Mapping Techniques.” In *The 4th International Symposium on Computer Mapping and GIS for Coastal Zone Management*. Scotia. https://doi.org/10.1201/9781420023428-9.
25. Li, Rongxing, Sagar Deshpande, Xutong Niu, Feng Zhou, Kaichang Di, and Bo Wu. 2008. “Geometric Integration of Aerial and High-Resolution Satellite Imagery and Application in Shoreline Mapping.” Marine Geodesy 31 (3): 143–59. https://doi.org/10.1080/01490410802265310.
26. Li, Rongxing, Jung Kuan Liu, and Yaron Felus. 2001. “Spatial Modeling and Analysis for Shoreline Change Detection and Coastal Erosion Monitoring.” Marine Geodesy 24 (1): 1–12. https://doi.org/10.1080/01490410121502.
27. Li, Rongxing, Ruijin Ma, and Kaichang Di. 2002. “Digital Tide-Coordinated Shoreline.” Marine Geodesy 25 (1–2): 27–36. https://doi.org/10.1080/014904102753516714.
28. Lipakis, Michalis, Nektarios Chrysoulakis, and Yiannis Kamarianakis. 2005. “Shoreline Extraction Using Satellite Imagery.” *BEACHMED-e/OpTIMAL*, no. Beach Erosion Monitoring: 81–96.
29. Liu, Hongxing, Douglas Sherman, and Songgang Gu. 2007. “Automated Extraction of Shorelines from Airborne Light Detection and Ranging Data and Accuracy Assessment Based on Monte Carlo Simulation.” Journal of Coastal Research 23 (6): 1359–69. https://doi.org/10.2112/05-0580.1.
30. Lowe, Meagan K., Farrah Anis Fazliatul Adnan, Sarah M. Hamylton, Rafael C. Carvalho, and Colin D. Woodroffe. 2019. “Assessing Reef-Island Shoreline Change Using UAV-Derived Orthomosaics and Digital Surface Models.” Drones 3 (2): 1–19. https://doi.org/10.3390/drones3020044.

31. Luijendijk, Arjen, Gerben Hagenaars, Roshanka Ranasinghe, Fedor Baart, Gennadii Donchyts, and Stefan Aarninkhof. 2018. “The State of the World’s Beaches.” Scientific Reports 8 (1): 1–11. https://doi.org/10.1038/s41598-018-24630-6.
32. Makota, Vedast, Rose Sallema, and Charles Mahika. 2004. “Monitoring Shoreline Change Using Remote Sensing and GIS: A Case Study of Kunduchi Area, Tanzania.” Western Indian Ocean J. Mar. Sci. 3 (1): 1–10.
33. Mukhopadhyay, Anirban, Sandip Mukherjee, Samadrita Mukherjee, Subhajit Ghosh, Sugata Hazra, and Debasish Mitra. 2012. “Automatic Shoreline Detection and Future Prediction: A Case Study on Puri Coast, Bay of Bengal, India.” European Journal of Remote Sensing 45 (1): 201–13. https://doi.org/10.5721/EuJRS20124519.
34. Nassar, Karim, Wael Elham Mahmod, Hassan Fath, Ali Masria, Kazuo Nadaoka, and Abdelazim Negm. 2019. “Shoreline Change Detection Using DSAS Technique: Case of North Sinai Coast, Egypt.” Marine Georesources and Geotechnology 37 (1): 81–95. https://doi.org/10.1080/1064119X.2018.1448912.
35. Natesan, Usha, N. Thulasiraman, K. Deepthi, and K. Kathiravan. 2013. “Shoreline Change Analysis of Vedaranyam Coast, Tamil Nadu, India.” Environmental Monitoring and Assessment 185 (6): 5099–5109. https://doi.org/10.1007/s10661-012-2928-y.
36. Niya, Ali Kourosh, Ali Asghar Alesheikh, Mohsen Soltanpor, and Mir Masoud Kheirkhahzarkesh. 2013. “Shoreline Change Mapping Using Remote Sensing and GIS, Case Study: Bushehr Province.” International Journal of Remote Sensing Applications 3 (3): 102–7.
37. Oyedotun, Temitope D. Timothy, Arturo Ruiz-Luna, and Alma G. Navarro-Hernández. 2018. “Contemporary Shoreline Changes and Consequences at a Tropical Coastal Domain.” Geology, Ecology, and Landscapes 2 (2): 104–14. https://doi.org/10.1080/24749508.2018.1452483.
38. Pajak, Mary Jean, and Stephen Leatherman. 2002. “The High Water Line as Shoreline Indicator.” Journal of Coastal Research 18 (2): 329–37.
39. Quante, Markus, and Franciscus Colijin. 2016. *North Sea Region Climate Assessment (NOSCCA)*. https://doi.org/10.1007/978-3-319-39745-0.
40. Quashigah, Philip Neri, Kwasi Appeaning Addo, and Kufogbe Sosthenes Kodzo. 2013. “Medium Resolution Satellite Imagery as a Tool for Monitoring Shoreline Change. Case Study of the Eastern Coast of Ghana.” Journal of Coastal Research, no. 65: 511–16. https://doi.org/10.2112/SI65-087.1.
41. Sesli, Faik Ahmet, Fevzi Karsli, Ismail Colkesen, and Nihat Akyol. 2009. “Monitoring the Changing Position of Coastlines Using Aerial and Satellite Image Data: An Example from the Eastern Coast of Trabzon, Turkey.” Environmental Monitoring and Assessment 153 (1–4): 391–403. https://doi.org/10.1007/s10661-008-0366-7.
42. Survey Department of Sri lanka. 2007. *National Atlas of Sri Lanka*. 2nd ed. Colombo: Survey Department of Sri Lanka.
43. Terefenko, Paweł, Dominik Paprotny, Andrzej Giza, Oswaldo Morales-Nápoles, Adam Kubicki, and Szymon Walczakiewicz. 2019. “Monitoring Cliff Erosion with LiDAR Surveys and Bayesian Network-

Based Data Analysis." Remote Sensing 11 (7): 1–16. https://doi.org/10.3390/RS11070843.

44. Toure, Seynabou, Oumar Diop, Kidiyo Kpalma, and Amadou Seidou Maiga. 2019. "Shoreline Detection Using Optical Remote Sensing: A Review." ISPRS International Journal of Geo-Information 8 (2). https://doi.org/10.3390/ijgi8020075.
45. Warnasuriya, T. W.S., Kuddithamby Gunaalan, and S. S. Gunasekara. 2018. "Google Earth: A New Resource for Shoreline Change Estimation—Case Study from Jaffna Peninsula, Sri Lanka." Marine Geodesy 41 (6): 546–80. https://doi.org/10.1080/01490419.2018.1509160.
46. Warnasuriya, T. W.S., M. P. Kumara, S. S. Gunasekara, K. Gunaalan, and R. M.R.M. Jayathilaka. 2020. "An Improved Method to Detect Shoreline Changes in Small-Scale Beaches Using Google Earth Pro." Marine Geodesy 43 (6): 541–72. https://doi.org/10.1080/01490419.2020.1822478.
47. Warnasuriya, T.W.S., P.B.T.P Kumara, and Niranga Alahacoon. 2014. "Mapping of Selected Coral Reefs in Southern, Sri Lanka Using Remote Sensing Methods." Sri Lanka Journal of Aquatic Sciences 19: 41–55. https://doi.org/10.4038/sljas.v19i0.7450.
48. White, Kevin, and Hesham M. El Asmar. 1999. "Monitoring Changing Position of Coastlines Using Thematic Mapper Imagery, an Example from the Nile Delta." Geomorphology 29 (1–2): 93–105. https://doi.org/10.1016/S0169-555X(99)00008-2.
49. Yao, Fang, Christopher E. Parrish, Shachak Pe'eri, Brian R. Calder, and Yuri Rzhanov. 2015. "Modeling Uncertainty in Photogrammetry-Derived National Shoreline." Marine Geodesy 38 (2): 128–45. https://doi.org/10.1080/01490419.2014.957792.
50. Yasir, Muhammad, Hui Sheng, Hong Fan, Shah Nazir, Abdoul Jelil Niang, Md Salauddin, and Sulaiman Khan. 2020. "Automatic Coastline Extraction and Changes Analysis Using Remote Sensing and GIS Technology." IEEE Access 8: 180156–70. https://doi.org/10.1109/ACCESS.2020.3027881.
51. Zagórski, Piotr, Kamila Jarosz, and Józef Superson. 2020. "Integrated Assessment of Shoreline Change along the Calypsostranda (Svalbard) from Remote Sensing, Field Survey and GIS." Marine Geodesy 43 (5): 433–71. https://doi.org/10.1080/01490419.2020.1715516.

Figures

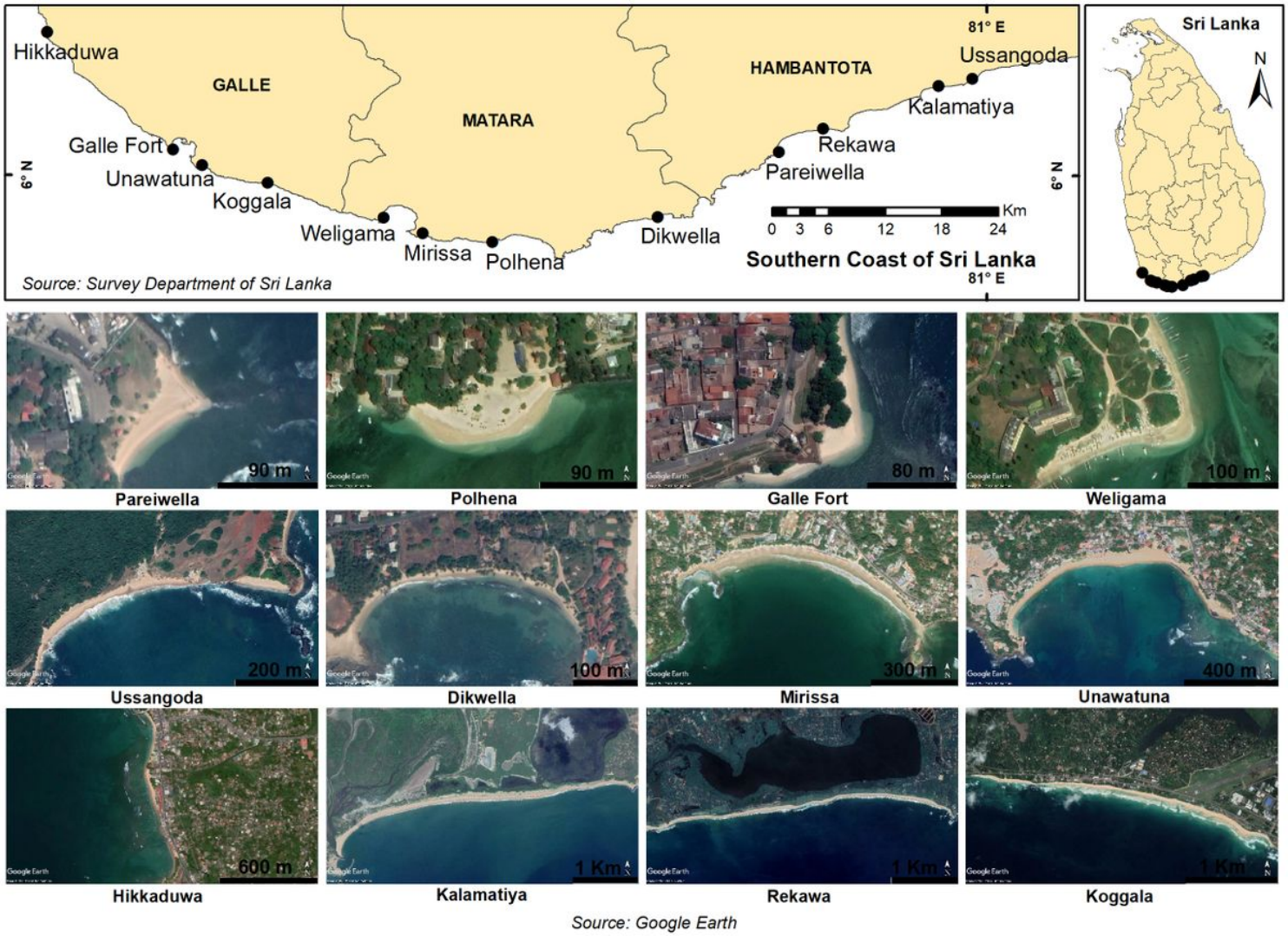

Figure 1

Study area

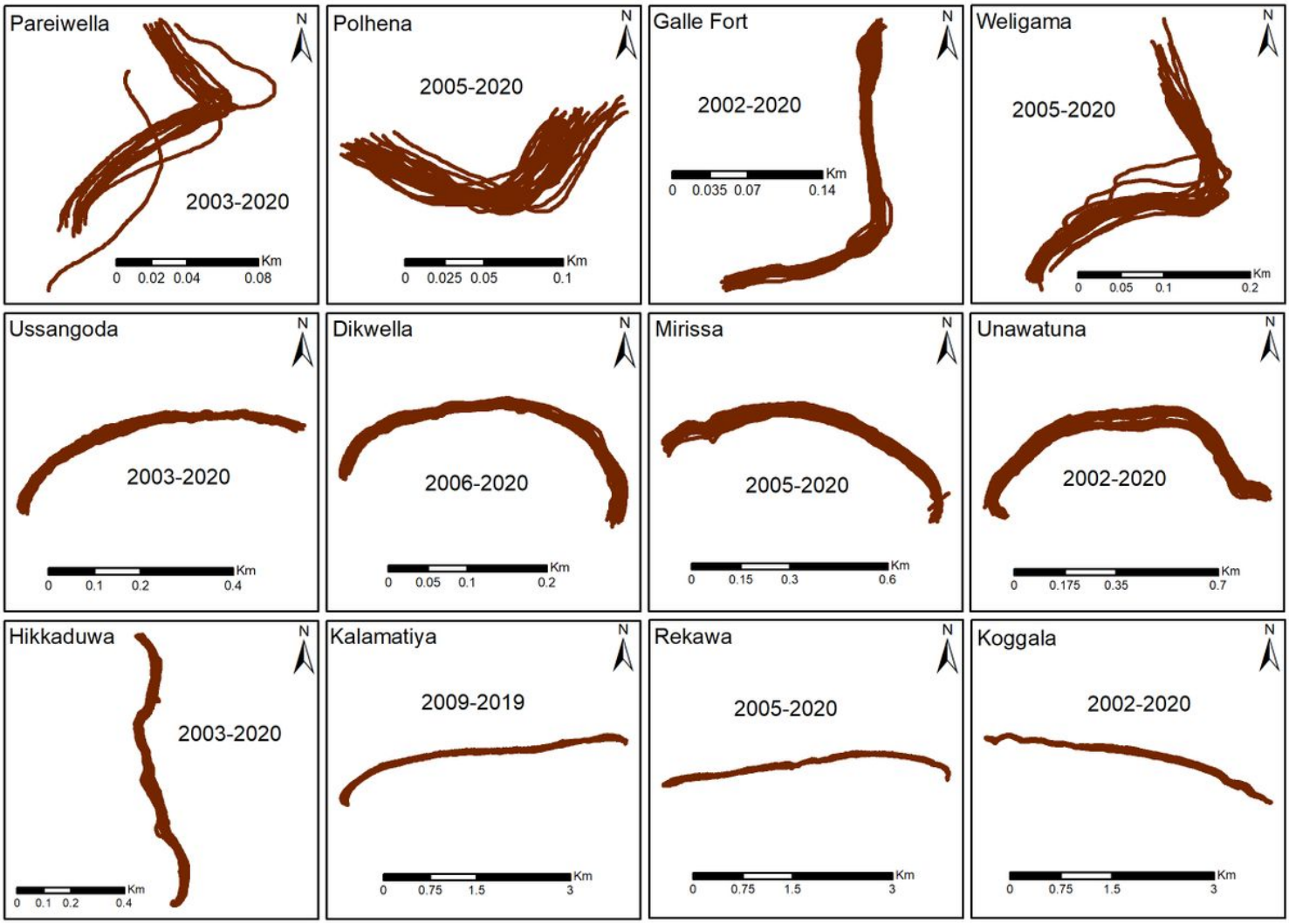

Figure 2

Beach morphology and shoreline distribution patterns

Note: Most appropriate shape under full extent was used to classify beaches through visual interpretation on high-resolution satellite images on Google Earth Pro

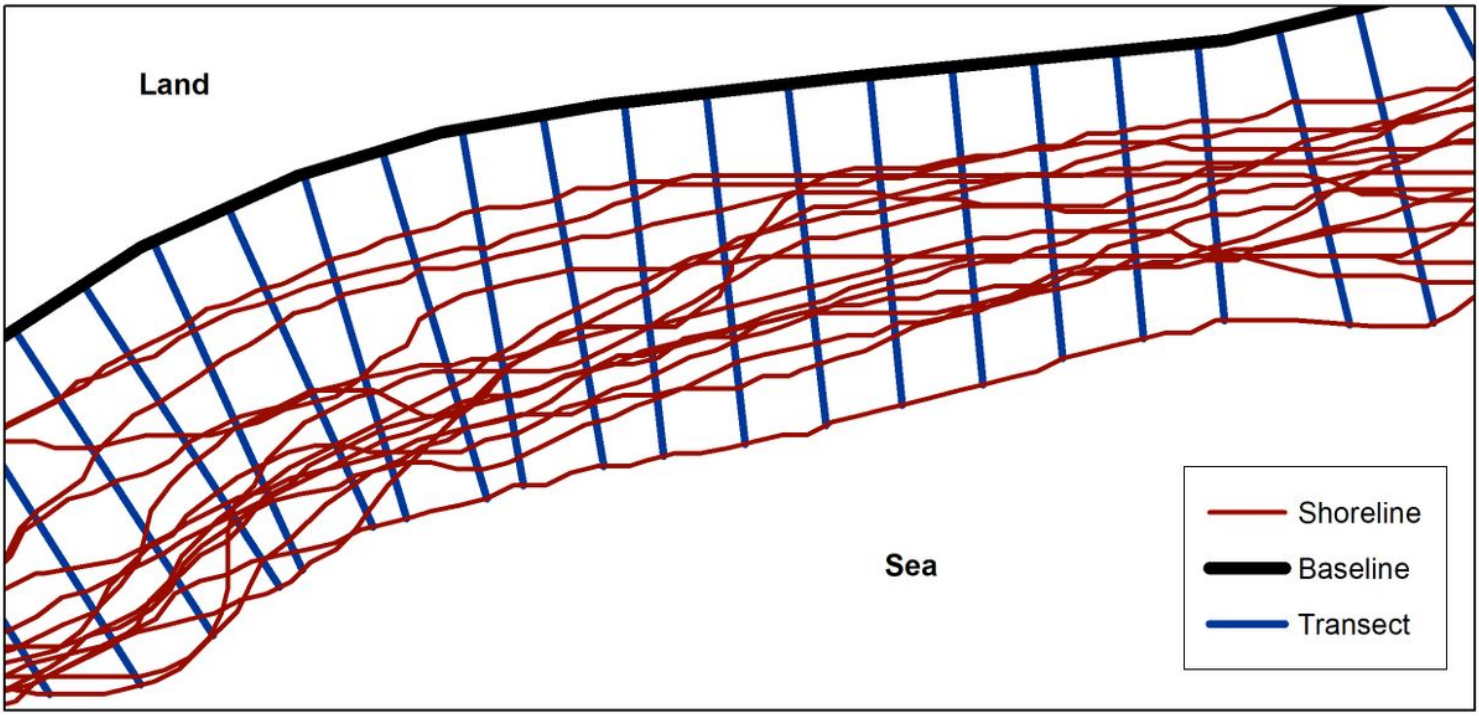

Figure 3

Shorelines, baseline and transects arrangement (example)

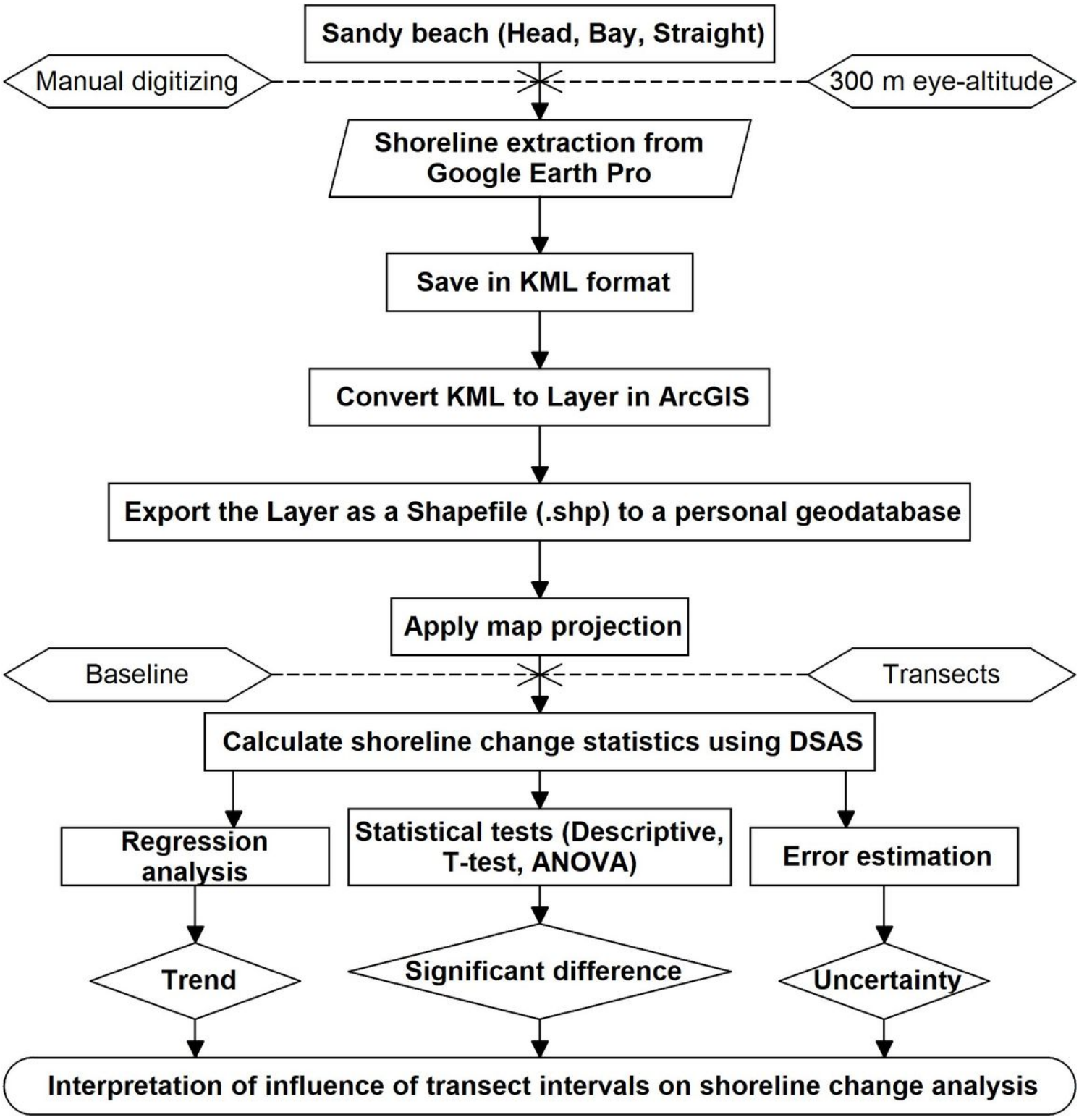

Figure 4

Flow chart of the methodology

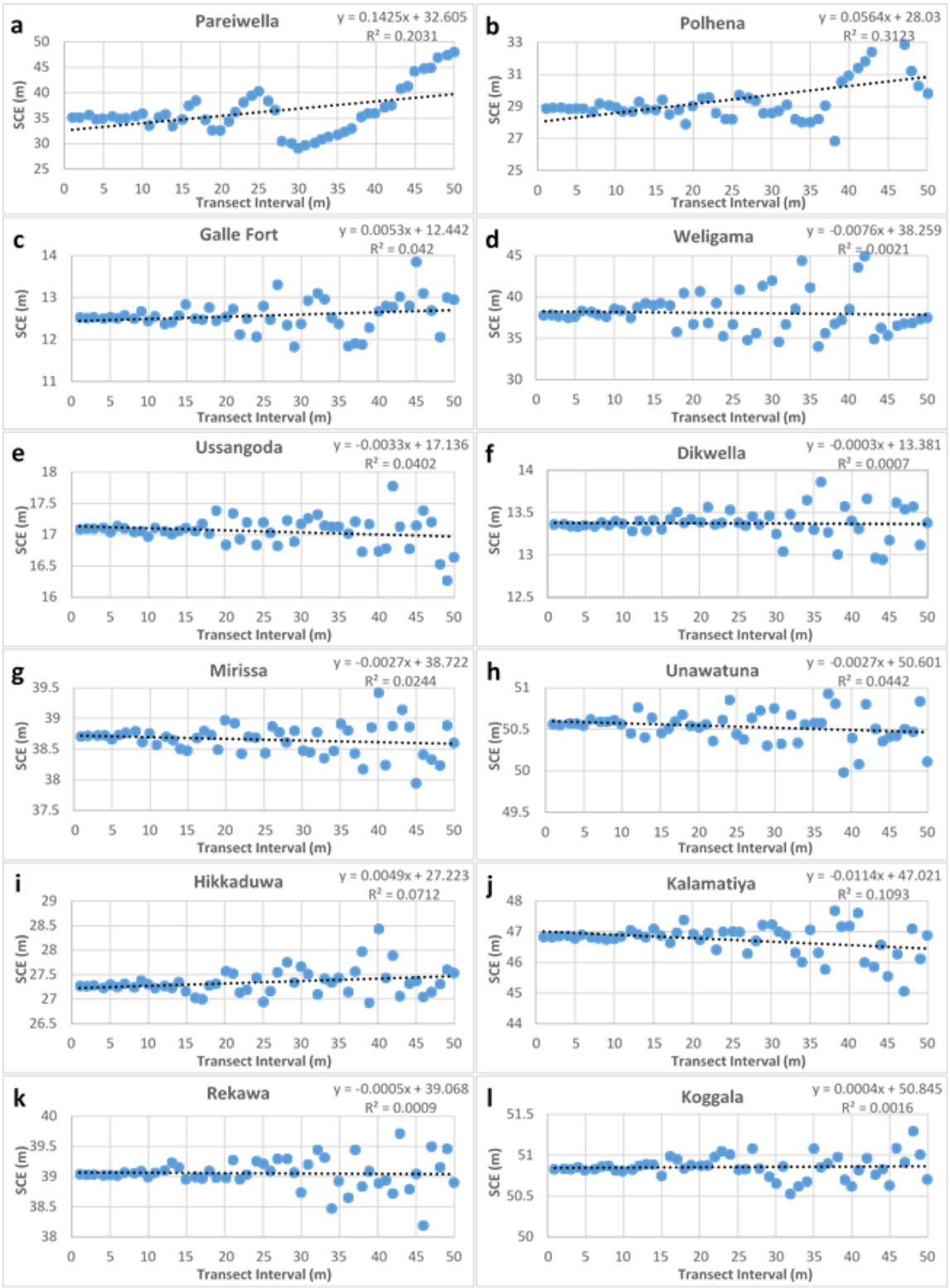

Figure 5

Average SCE against TISs for each beach

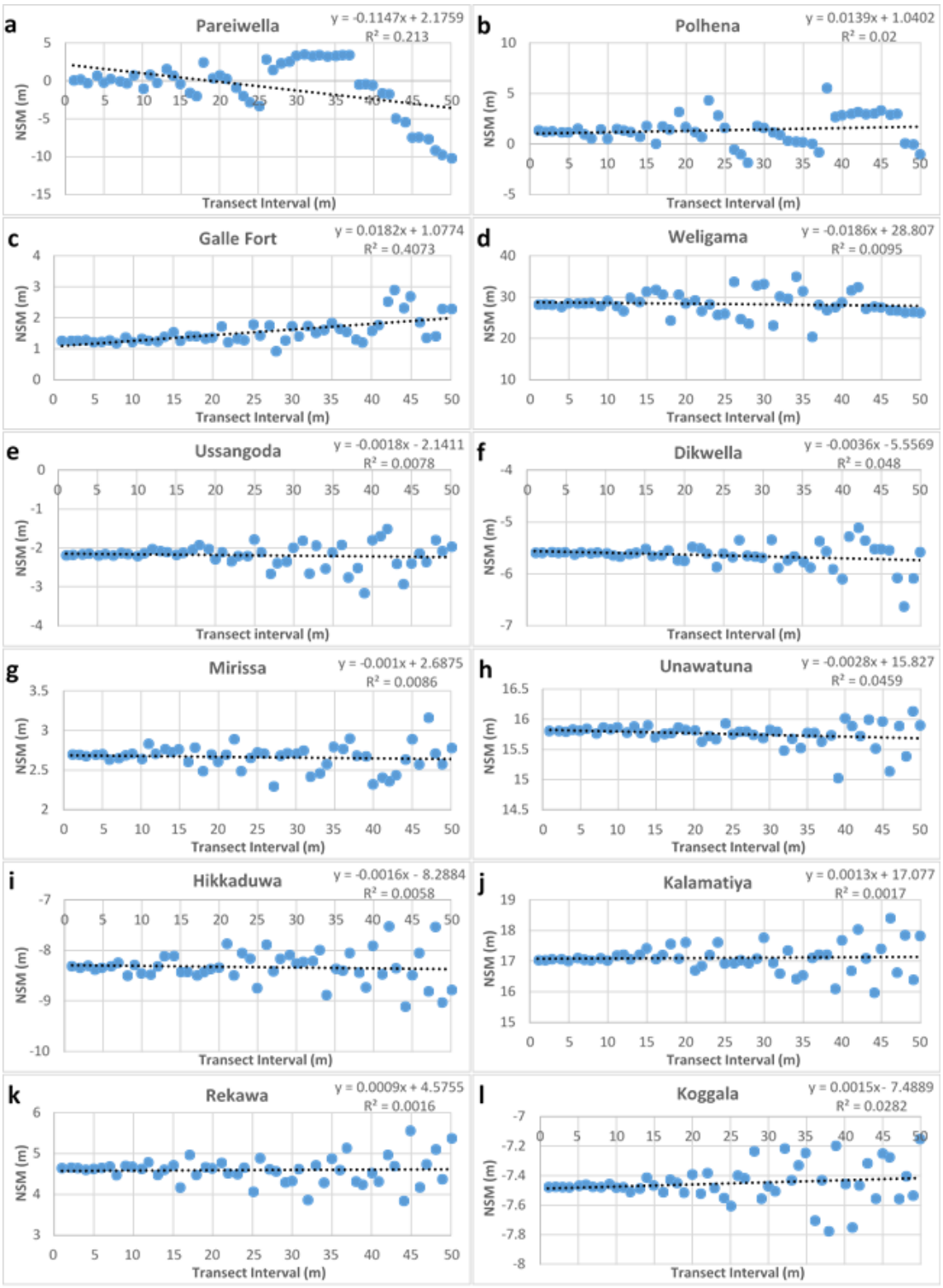

Figure 6

Average NSM against TISs for each beach

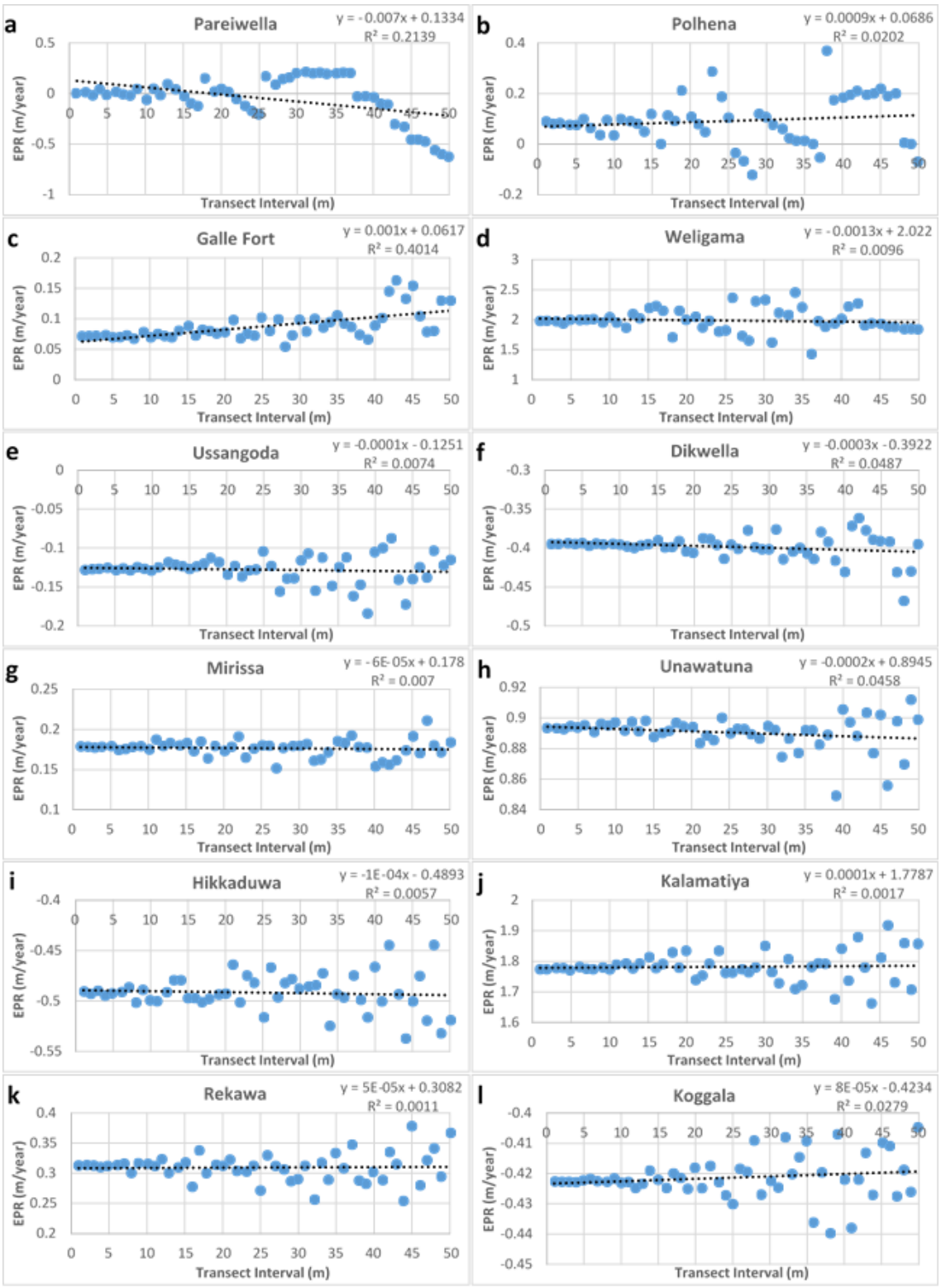

Figure 7

Average EPR against TISs for each beach

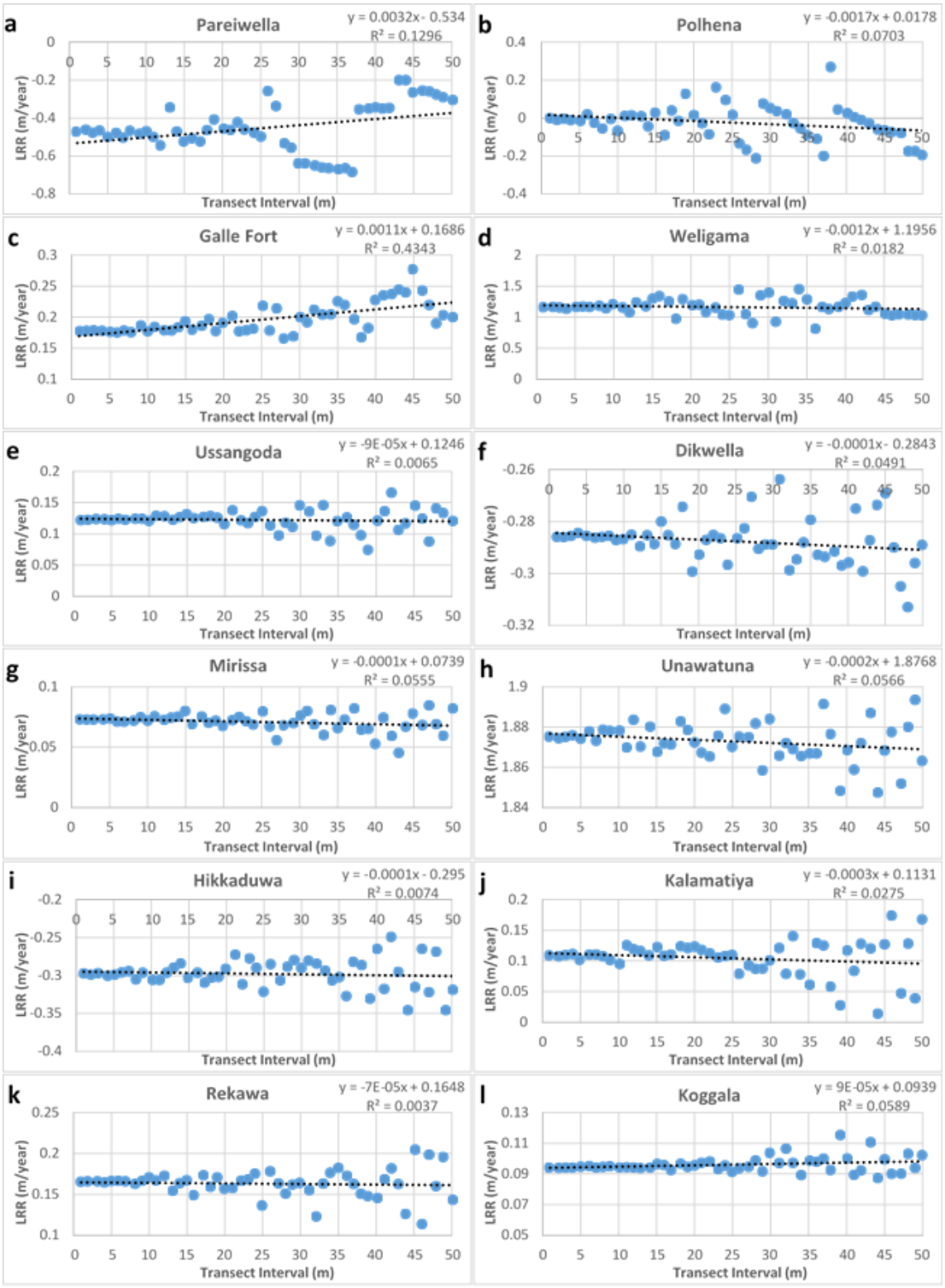

Figure 8

Average LRR against TISs for each beach

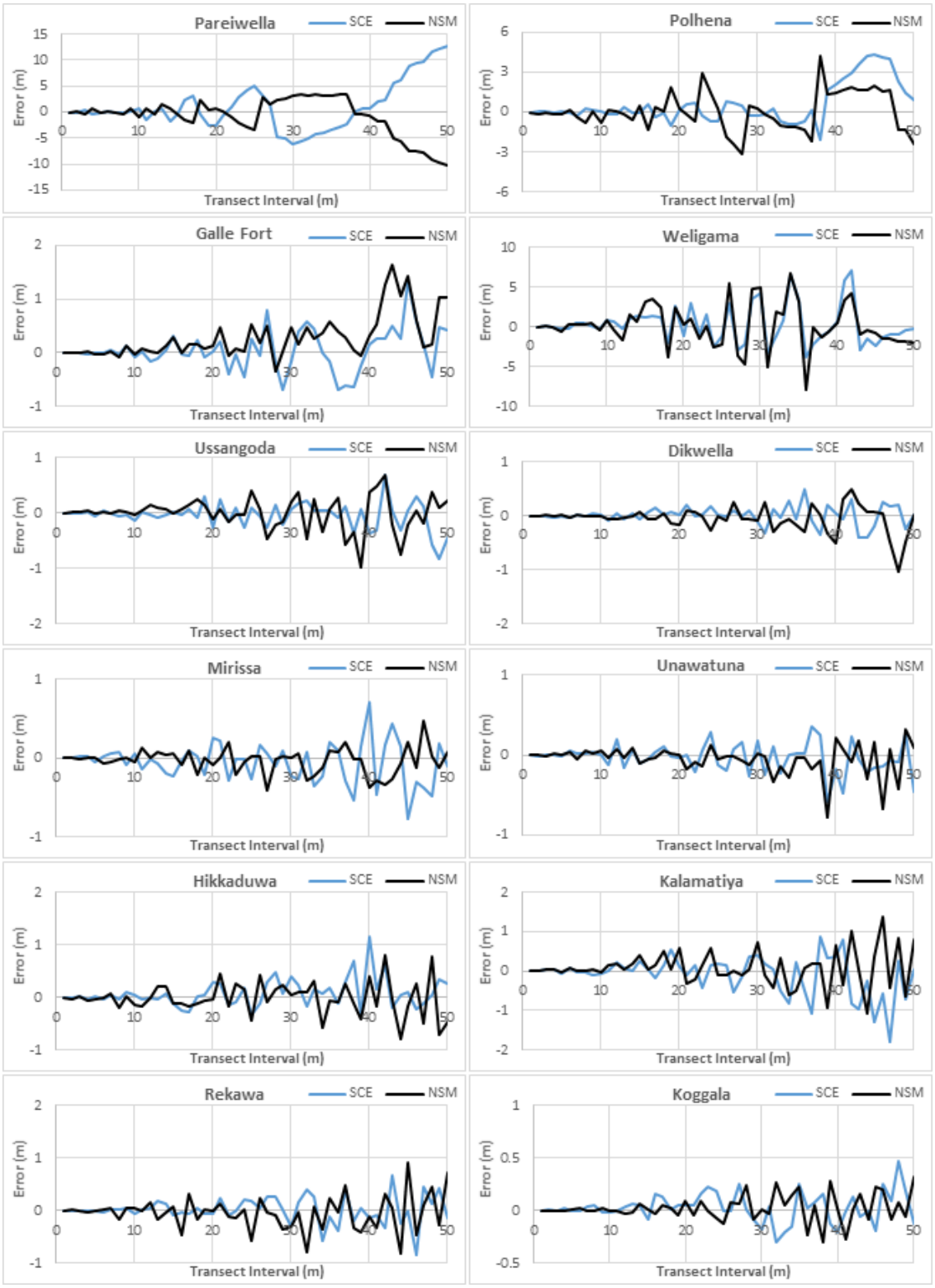

Figure 9

TIE against TIS (SCE and NSM)

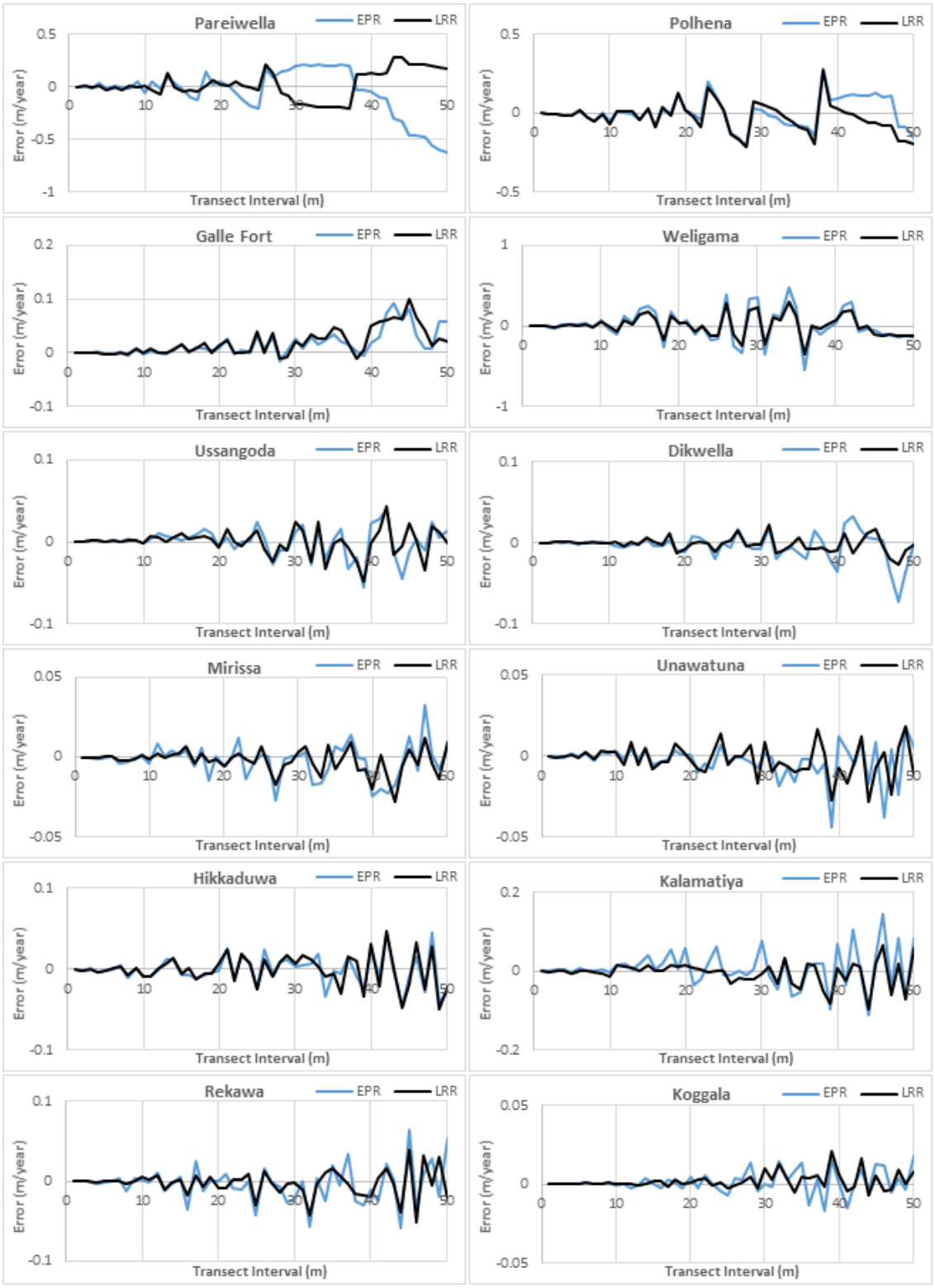

Figure 10

TIE against TIS (EPR and LRR)